Pergamon

PII: S0191–8141(98)00003–0

Journal of Structural Geology, Vol. 20, No. 6, pp. 783 to 798, 1998

0191-8141/98 $19.00 + 0.00

Ductile deformation of tonalite in the Suomusjärvi shear zone, south-western Finland

HARRIET LONKA

Department of Geology, Helsinki University, Finland

and

KAREL SCHULMANN and ZDENĚK VENERA

Institute of Petrology and Structural Geology, Faculty of Science, Charles University, Czech Republic

(*Received* 17 *January* 1997; *accepted in revised form* 8 *November* 1997)

Abstract—Different states of deformation of tonalite with a weak original contiguity of plagioclase were studied in the Suomusjärvi shear zone, south-western Finland. Weakly deformed tonalite is characterised by strain concentration in a conjugate network of narrow shears. Quartz and biotite deformed by crystal plasticity while plagioclase shows extensive fracturing. An interconnected weak layer structure is typical for this stage of deformation, with a densely packed strong phase, a relatively small proportion of weak matrix and a high competence contrast between the strong and weak phases. A high concentration of stress and strain rate in weak minerals produced continuous fracturing of relict plagioclase grains. This deformation stage was not accompanied by changes in the bulk chemistry of the rock.

Increasing deformation led to a major change in deformation mechanism, expressed by granular flow in the ductile matrix and rigid body rotation of ovoid feldspar crystals. The size of the plagioclase crystals decreased by a combination of dynamic recrystallisation and chemical dissolution. This strain stage was also associated with fluid infiltration into the progressively narrowing shear zone. A steady-state fabric was probably attained in the core of the shear zone, which is characterised by a decrease in grain size and plagioclase aspect ratio, and a loss of shape-preferred orientation. A low stress concentration in a weak matrix in dynamic equilibrium is consistent with the proportion of relict plagioclase and size of the ovoid grains. © 1998 Elsevier Science Ltd. All rights reserved

INTRODUCTION

It is generally accepted that various states of rock transformation can be related to shear zone strain gradients and correspond to evolving stages in the deformation history (Means, 1995). Hull (1988) and Mitra (1992) divide shear zones into three groups with the following end members: (1) Type I zones which thicken with time due to work hardening and (2) type II zones that become narrower with time because of strain softening. The latter shear zone type is a relatively reliable recorder of rock deformation history because the highly strained shear zone interior passed through the low-strain stage preserved at the shear zone margin (Means, 1995).

Strain localisation in ductile shear zones of type II is controlled by the physical conditions of deformation (pressure, temperature, fluid pressure), rock composition and bulk intensity of deformation. In deformed monomineralic rocks, the strain softening is due to changes in deformation mechanism such as continuous recrystallisation (White *et al*., 1980; Schmid, 1982). In polymineralic rocks, however, the contrasting strength of minerals constituting the rocks leads to distinct deformation mechanisms in different minerals. Consequently, microstructures developed across the deformation gradient in ductile shear zones in granitic rocks have been the subject of many deformation studies (e.g. Burg and Laurent, 1978; Mitra, 1978; Schulmann *et al*., 1996). Strain softening is strongly controlled by the proportion of the interconnected weak mineral (Jordan, 1987, 1988) and the rheological contrast between individual minerals constituting the rock (Handy, 1990, 1994).

At weak strains the deformation is supported by a framework of strong minerals that shield the weak phase. The rock is deformed more or less homogeneously resulting in formation of a so-called load-bearing framework (LBF) structure (Handy, 1990). With increasing deformation the LBF structure collapses and narrow, commonly conjugate shear instabilities develop in weak minerals. This interconnected weak layer (IWL) is not stable either and changes with increasing strain (Jordan, 1987; Schulmann *et al*., 1996), resulting in the development of a differentiated layering.

The objective of this study is to show progressive greenschist grade mylonitisation of tonalite in a shear zone in which the strong phase does not form a contiguous framework. An attempt is made to describe the mechanical development of a polyphase system characterised by an increase in the proportion of matrix associated with changes in the main deformation mechanisms. Finally, we attempt to show that steady-

state flow conditions were attained in the core of the shear zone.

GEOLOGICAL SETTING

The two major geological units of the Precambrian bedrock in southern Finland are the Archean basement (2.9–2.6 Ga) and the early Proterozoic Svecokarelian terrane (2.0–1.8 Ga). The latter is divided into the intracratonic Karelian domain and the orogenic Svecofennian domain (Gaál and Gorbatschev, 1987). The Svecofennian domain consists of metasedimentary and metavolcanics rocks intruded by large volumes of granitoids. The supracrustals of the Svecofennian domain are further divided into North, Central and South Svecofennian subprovinces. The South Svecofennian Subprovince consists mostly of migmatitic metaturbidites intercalated with metavolcanic rocks of mainly intermediate composition (Schreurs and Westra, 1986; Gaál and Gorbatschev, 1987).

The West Uusimaa region, in which the present study area is located is a part of the South Svecofennian Subprovince (Fig. 1), consisting mostly of volcanic–sedimentary rocks intruded by synorogenic gabbro–tonalite–granodiorite rocks. The zircon ages of these igneous rocks are approximately 1.89 Ga (Huhma, 1986). The intrusion of late orogenic K-rich granites occurred 1.83 Ga ago, and was associated with extensive migmatisation. The West Uusimaa area is characterised by a prograde metamorphic history reaching amphibolite to granulite facies metamorphism, with the degree of metamorphism increasing towards the north-east (Schreurs and Westra, 1986).

Three separate deformation phases can be recognised in the West Uusimaa area and the adjacent supracrustal rocks (Schreurs and Westra, 1986; Ploegsma, 1989). The earliest F_2 folding and associated transposed S_0–S_1 metamorphic layering, which retains a subhorizontal attitude, is possibly related to the earliest stages of thrusting. These structures are only found in better preserved domains outside the West Uusimaa area. The prevailing structure in the study area is instead represented by a subvertical S_2 foliation and locally by D_2 shear zones which exhibit annealed textures in this sector. Both phases of deformation described above took place during prograde metamorphism and are associated with compressional tec-

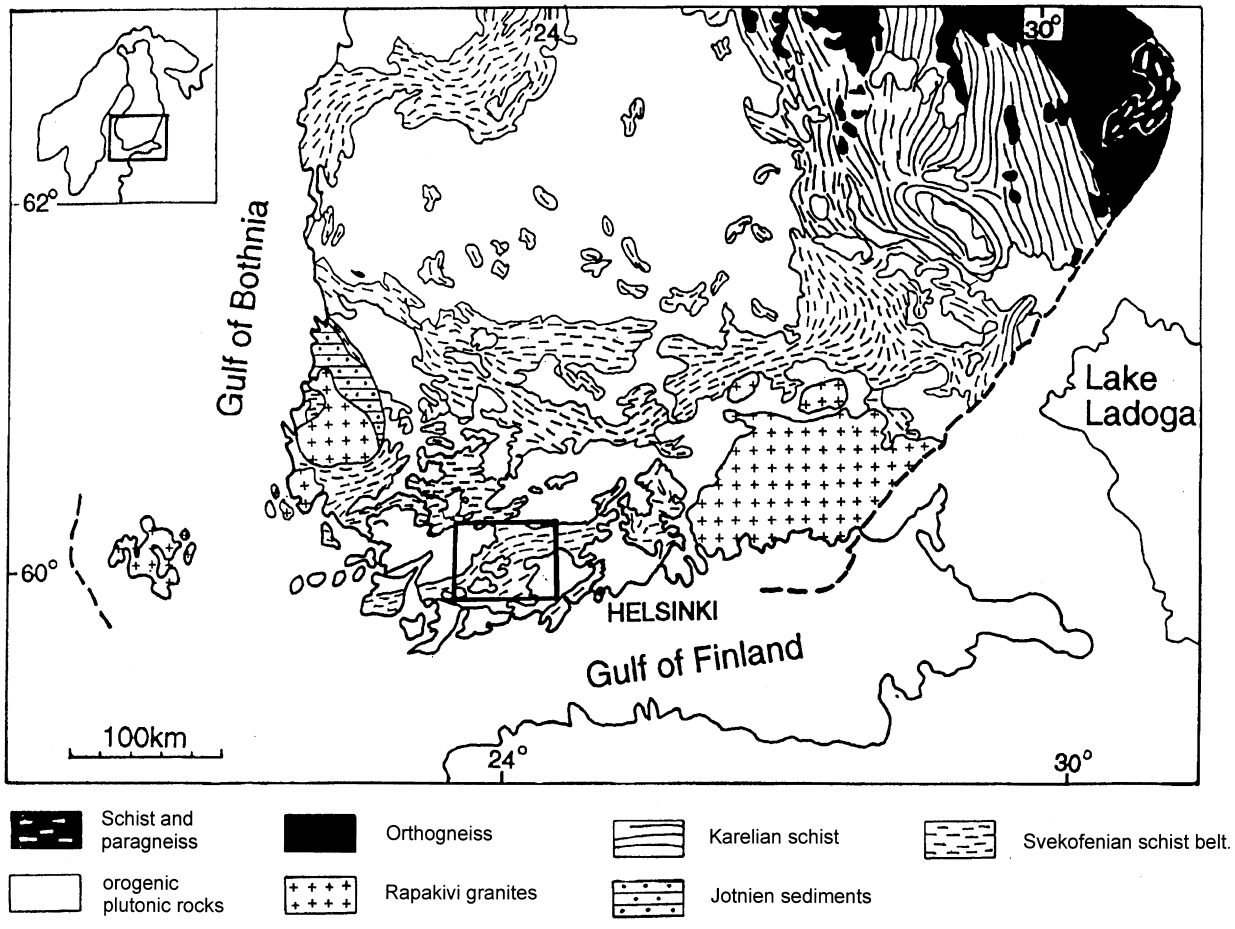

Fig. 1. Geological map of southern Finland. Area outlined by the box refers to map in Fig. 2(a).

tonics (Ploegsma, 1989). Internal magmatic planar structures within the tonalite body are concordant with the regional D_2 structural pattern. This suggests syntectonic emplacement of the tonalite body during D_2 deformation, which coincides with the regional peak of metamorphism.

Late vertical shear zones are the salient feature of the D_3 greenschist facies deformation phase (Ploegsma, 1989). The Suomusjärvi shear zone with which this paper is concerned, represents such a typical late shear zone. It is subvertical, NNE–SSW striking and is subparallel to the regional S_2 foliation (Fig. 2). This shear zone is represented by a 5 m thick zone of ultramylonite developed along the eastern margin of the tonalite body. The mylonitic foliation inside the shear zone bears a subvertical stretching lineation, and sense-of-shear criteria indicate an upward movement of the eastern block (Ploegsma, 1989).

MICROSTRUCTURAL EVOLUTION

The tonalite affected by the Suomusjärvi shear zone records several stages of mylonite evolution ranging from virtually undeformed rock to ultramylonite. The amount of matrix was used as a criterion for a purely descriptive classification of the degree of mylonitisation (Schmid and Handy, 1991) and in the following figures we denote samples of protomylonite, mylonite and ultramylonite with capitals A, B, C, respectively.

Stage I—protolith tonalite

The protolith is characterised by a magmatic fabric (Fig. 3a) and is composed of plagioclase An_{30} (45–55%), quartz (25–30%) and biotite (20–30%) (Fig. 4a).

Plagioclase occurs as euhedral to subhedral grains up to 5 mm in size exhibiting a strong preferred orien-

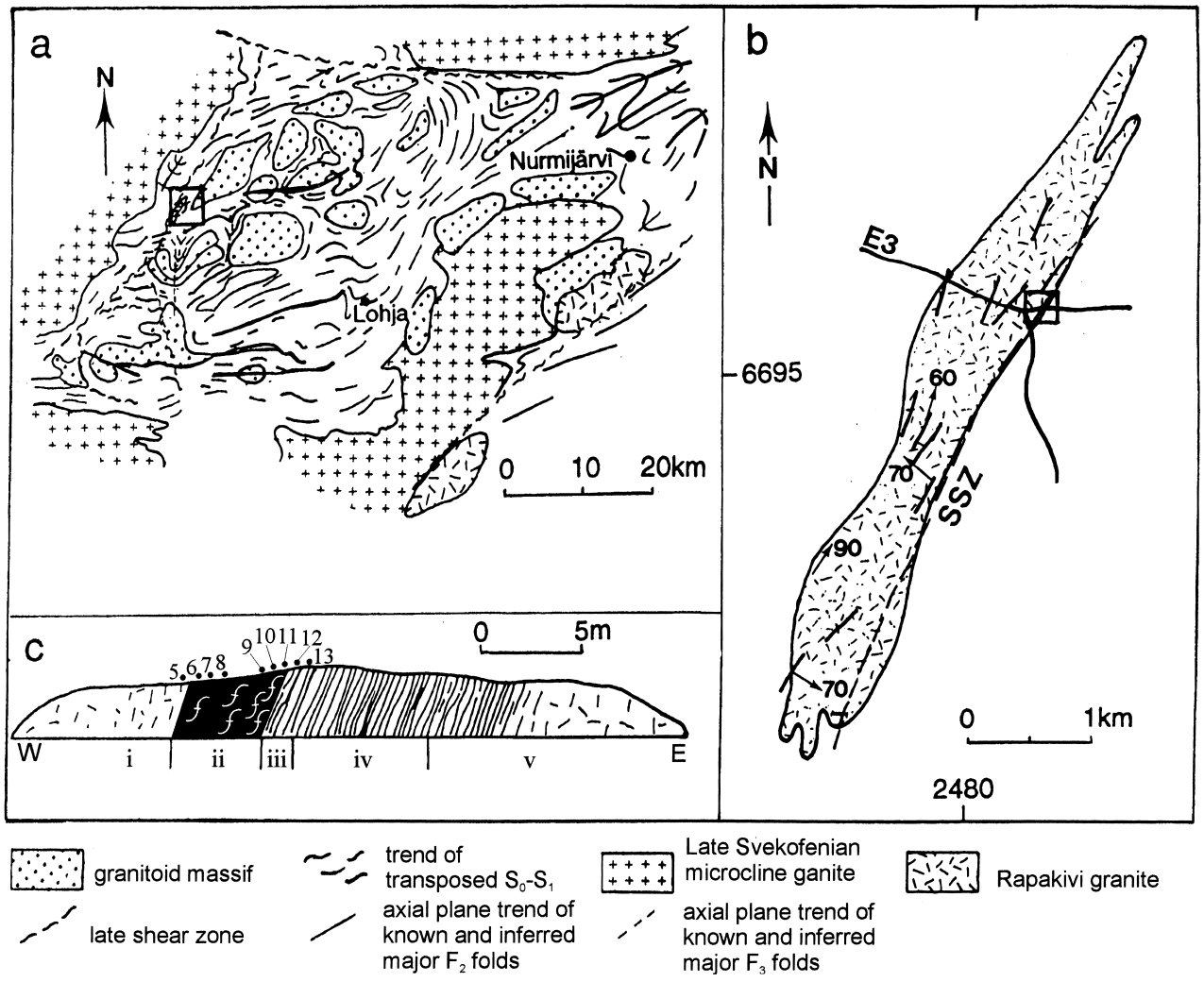

Fig. 2. Geology of the West Uusimaa area. (a) Geological map of the West Uusimaa area, the box indicating the location of the Suomusjärvi tonalite. (b) Schematic map of the Suomusjärvi tonalite showing strike of subvertical mylonitic foliation and trend of L_3 stretching lineation. SSZ—Suomusjärvi shear zone. (c) Sketch of a roadcut across the Suomusjärvi shear zone composed of the following sections: (i) incipiently foliated tonalite, (ii) mylonite and ultramylonite, (iii) foliated tonalite, (iv) mylonitic metapelites, (v) transition of granite into orthogneiss. Sample locations and numbers are indicated.

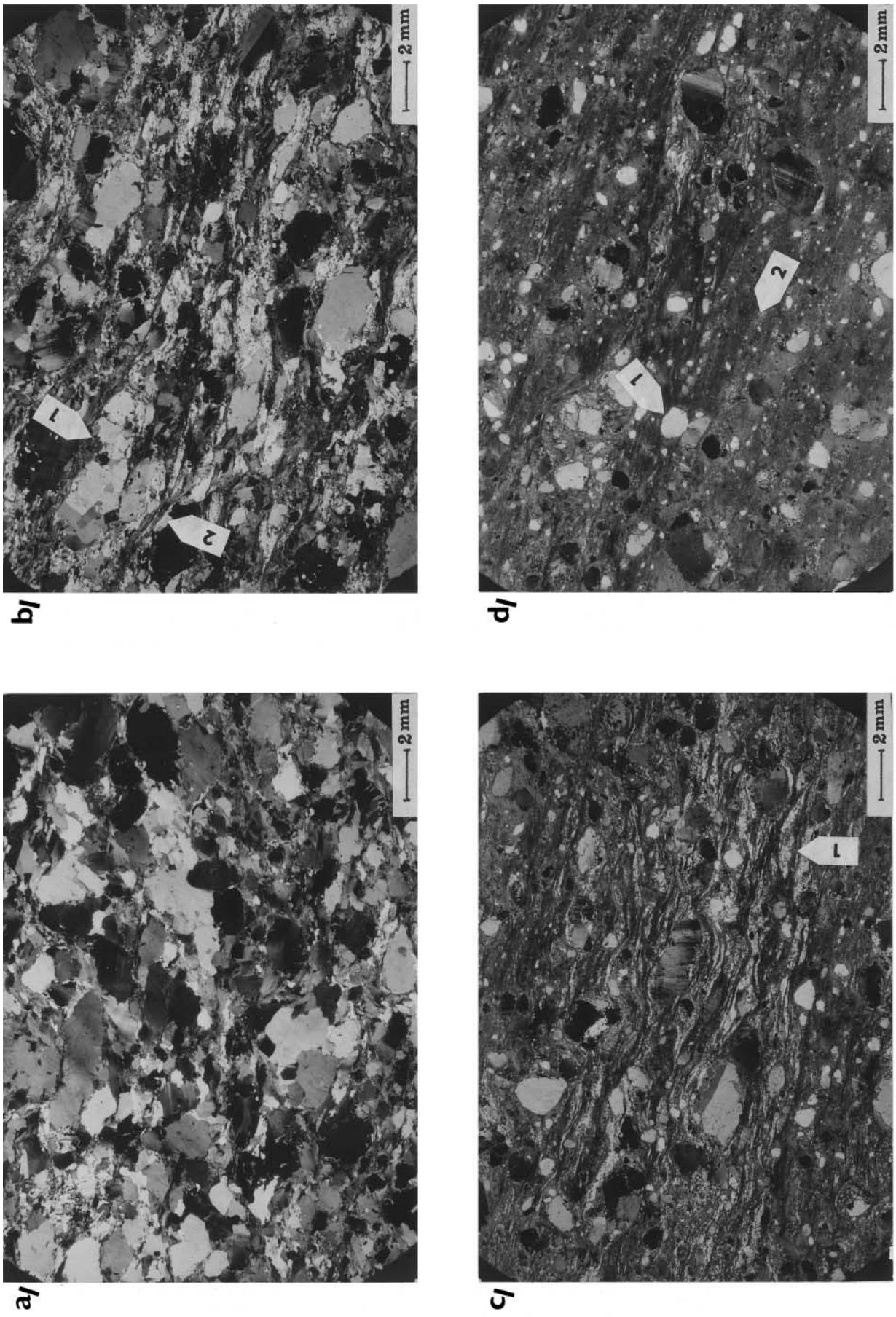

Fig. 3. Microstructural evolution across the shear zone in four stages. (a) Tonalite at the margin of the shear zone shows obvious primary preferred orientation of plagioclase phenocrysts, micas and quartz grains. (b) Protomylonite exhibits strong deformation localized in quartz and biotite (arrow 2). Note fracturing of plagioclase (arrow 1). (c) Mylonite characterised by increasing amount of weak matrix. Quartz ribbons (arrow 1) wrapped around plagioclase clasts. (d) Ultramylonite is marked by total conversion of quartz, biotite and plagioclase into fine-grained matrix, heterogeneous in colour (arrow 2). Rounded relics of feldspar phenocrysts (arrow 1) passively float in the matrix.

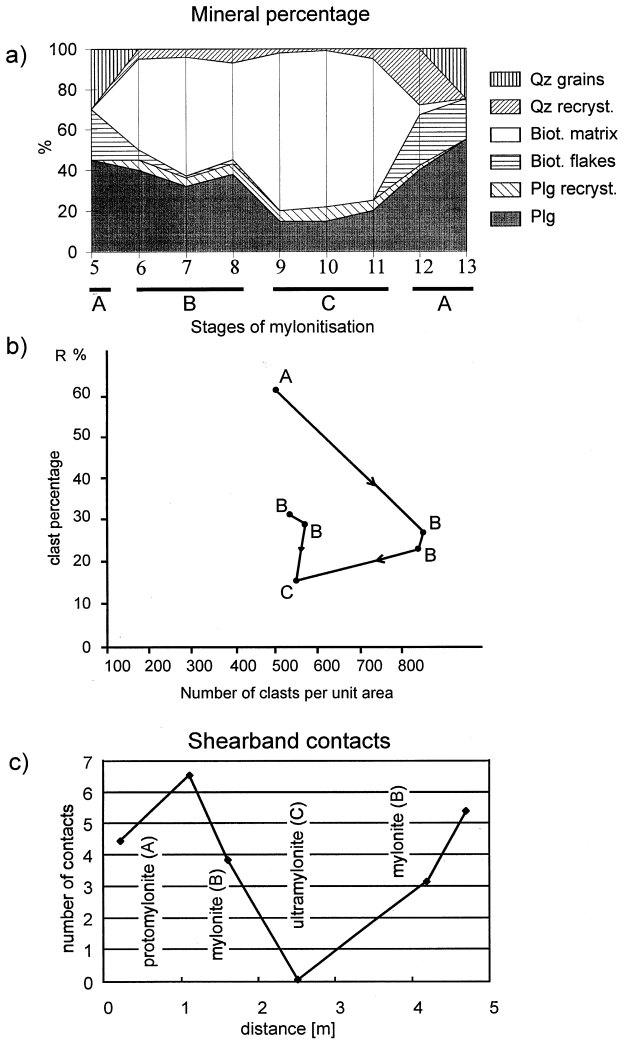

Fig. 4. (a) Profile of mineral percentages across the shear zone indicating a rapid disappearance of original quartz, biotite and plagioclase in favour of matrix material. Modal analyses: 5, 12, 13—protomylonitic tonalite; 6, 7, 8—mylonite; 9, 10, 11—ultramylonite. Letters A, B, C indicate groups of samples corresponding to stages of mylonitisation (protomylonite–mylonite–ultramylonite) described in other figures. (b) Diagram showing relationship between number of clasts per unit area and clast percentage. (c) Diagram showing number of shear band connections per square centimetre through the shear zone, see Marquer (1989) for counting method description.

tation. These grains show weak undulatose extinction and ubiquitous twinning according to albite and pericline laws. Submagmatic fractures in plagioclase forming acute angles to the (010) planes are filled with quartz or biotite.

Biotite forms large flakes up to 2 mm in size often surrounding plagioclase grains. It also shows a well-developed preferred orientation and in some cases exhibits undulatose extinction (Fig. 5a). Quartz forms large blebs, from 2 to 5 mm in size, generally elongated parallel to the foliation trace. It exhibits prismatic subgrains often parallel to the grain elongation or chess-board undulatose extinction (Fig. 5a). All these observations are consistent with microstructure development near the solidus boundary of tonalitic magma and indicate transition from magmatic to solid state deformation (Blumenfeld *et al.*, 1986; Melka *et al.*, 1992).

Stage II—protomylonite (10–20% recrystallised matrix)

The protomylonite consists of quartz (20–30%), feldspar (45–55%) clasts, a mosaic of recrystallised feldspar (5%) and biotite clasts (10%). The extremely fine-grained dark biotite matrix reaches a maximum of 20% of the total rock volume (Fig. 4a). The rock contains 60% plagioclase clasts with a density of about 500 clasts per 3 cm^2 (Fig. 4b). The most important feature of the beginning of tonalite deformation is the development of an anastomosing network of synthetic and antithetic shears (Gapais, 1989b) which affect predominantly biotite and quartz (Fig. 4c). In contrast, plagioclase is relatively shielded from deformation (Fig. 3b). Plagioclase is present in the form of large elongate clasts up to 5 mm in size with aspect ratios varying between 2 and 6. Its grains exhibit undulatose extinction and strain-induced twinning (Fig. 5b), with both cleavage planes and twins commonly bent. Large grains are affected by an irregular network of fractures accompanied by the development of strain-induced recrystallisation along clast margins and internal deformation bands. The optical microstructures include features typical of cataclastic flow and of dislocation creep (Tullis and Yund, 1987).

Biotite exhibits signs of plastic deformation associated with slip along the (001) plane, and kinking and recrystallisation along the margins (Fig. 5b). In zones of intense shear deformation, e.g. at the tips of shear bands or between feldspar clasts, the biotite is completely converted to an ultrafine dark matrix (Fig. 5b).

Quartz is strongly recrystallised and occurs in ribbons or aggregates consisting of relics of old grains and aggregates of recrystallised grains. The size of the latter varies between 10 and 50 μm, with the smallest occurring between closely spaced large feldspar clasts and with progressively larger grains occurring towards stress-protected areas with more widely spaced feldspars (Fig. 5c). Recrystallised grains are irregular in shape and have lobate (Fig. 5c) to straight boundaries indicating migration of grain boundaries (Urai *et al.*, 1986). In protected areas, mantle and core structures (White, 1976) are present. These microstructures indicate that recrystallisation originated through both migration recrystallisation and progressive sub-grain rotation (Hirth and Tullis, 1992).

Grain size variation along shear bands is attributed to local stress and strain gradients typical of an interconnected weak layer structure (IWL) characterised by a small proportion of the weak phase (Handy, 1990, 1994).

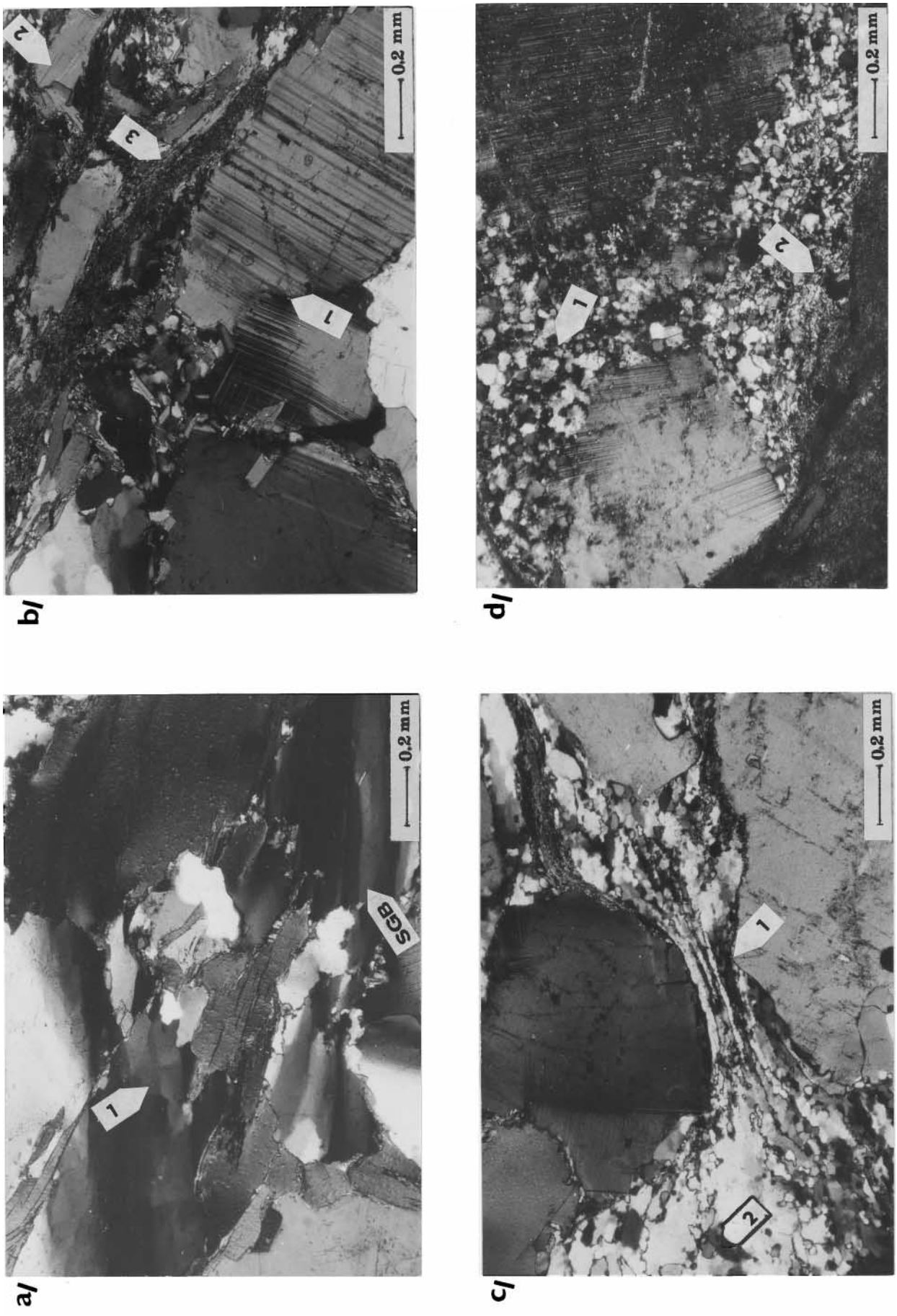

Fig. 5. Phenomena of deformation mechanisms in minerals of progressively deformed tonalite. (a) Tonalite. Prismatic subgrain boundaries (SGB) are subparallel to grain elongation and chessboard structures (arrow 1). (b) Stage II. Fracturing of plagioclase and deformation twinning (arrow 1), kinking of biotites (arrow 2) and ultrafine-grained matrix in shear zones (arrow 3). (c) Protomylonite. Grain size variation of quartz grains between feldspar clasts (arrow 1). Both rotation and migration recrystallisation mechanisms were active in stress protected zones (arrow 2). (d) Mylonite. Plastic deformation of plagioclase. New larger grains (arrow 1) are preserved in stress-protected zones while the smaller ones occur in stress exposed regions (arrow 2).

Stage III—mylonite (40–70% matrix)

This rock contains plagioclase clasts (30–40%), quartz (20%), biotite (10%) and ultrafine-grained matrix (40–50%) of variable composition with a grain size from 1 to 5 μm (Fig. 4). The volume of clasts decreases to 30–20% of the total rock, while the total number increases in some samples up to 800 per 3 cm^2 (Fig. 4b).

The deformation is concentrated in a network of anastomosing shear bands within a weak matrix (Fig. 4c). Relict quartz ribbons are passively wrapped around rigid clasts or in a weak matrix. Feldspar clasts are fractured and/or converted to elongate fine-grained monomineralic aggregates. This process is connected with an increase in the fine-grained feldspar matrix. Fractures within the relict plagioclase grains pass into wide microshear zones filled with a very fine-grained groundmass (10–20 μm) (Fig. 5d). The volume of quartz decreases at this stage of deformation (Figs 3c & 4a), and it appears as ribbons composed of fine recrystallised grains (10–30 μm) with straight boundaries and sub-equant shapes (Fig. 5e). Biotite is almost completely converted to fine-grained dark matrix, which includes remnants of recrystallised plagioclase and quartz.

The small variation in quartz grain size, the large number of ovoid clasts and the decreasing number of shear bands all indicate presence of an IWL structure characterised by a high proportion of weak matrix and high viscosity contrast between strong and weak phases (Handy, 1994).

Stage IV—ultramylonite

In the core of the mylonitic zone, the feldspar clasts decrease in number, size and volume, and the dark, fine-grained matrix comprises more than 70% of the total rock volume (Figs 3d & 4a). The volume of relict feldspar clasts is as low as 10–12%, while the number of clasts is about 500 per 3 cm^2, which is close to the clast number in the protomylonitic stage (Fig. 4b).

The fine-grained feldspar and quartz fractions almost disappear. Pressure protected sides of feldspars preserve remnants of fine-grained aggregates whereas domains exposed to higher stress areas exhibit sharp boundaries (Fig. 5f). Rounded, isolated feldspar clasts and sporadic polycrystalline grain aggregates flow freely in the fine grained matrix (Fig. 3d). Neither quartz nor biotite are microscopically recognisable. This stage represents a reduction in the number of shear bands to zero (Fig. 4c). The fine-grained matrix exhibits subparallel zones of different colours indicating the presence of mineral precursors. This stage of deformation is characterised by a clast/matrix IWL structure with a high viscosity contrast between relic feldspar and weak matrix.

GEOCHEMICAL PROFILE ACROSS THE SHEAR ZONE AND MINERAL CHEMISTRY

Syntectonic metamorphic reactions in deformed granites lead to destabilisation of feldspars and micas, to the formation of ultra-fine-grained matrix and to reaction softening in ductile shear zones (White *et al.*, 1980). The influence of deformation on changes in mineralogy and chemical mass transfer in ductile shear zones in quartzo-feldspathic rocks is attributed to shearing under low-grade metamorphic conditions (Mitra, 1978; Marquer, 1989). Chemical transfer in ductile shear zones is either controlled by chemical equilibrium of sheared rocks with external fluid in open system (Etheridge *et al.*, 1984) or by deformational mechanisms coupled with mineral transformations (White and Knipe, 1978). Chemical studies of ductile shear zones may help to answer the question as to whether deformed rock is softened exclusively by change in deformational mechanisms, by mineralogical changes associated with an influx of external fluids or by mineral transformations connected with retrograde thermal conditions (Marquer, 1989).

Shear bands—pathways for fluids?

Marquer (1989), Gapais (1989a) and Marquer and Burkhard (1992) have shown that heterogeneous shear band networks act as pathways for fluids in deformed granitic rocks. The number and length of shear bands is directly connected to the degree of chemical mass transfer and increases with increasing deformation intensity (Marquer, 1987, 1989).

The number of connections between heterogeneous shear bands (30–40 μm thick) cutting the matrix (Fig. 4c) has been calculated in the Suomusjärvi shear zone to test whether the shear bands acted as fluid pathways and contributed to reactional softening. The network of heterogeneous shear bands originated during the protomylonitic stage when the matrix volume exceeded 10%. With increasing deformation the number of shear bands increases. However, the transition from mylonite to ultramylonite is marked by a decrease in the number of shear band connections and, in the ultramylonite, the shear bands disappear entirely (Fig. 4c).

Bulk rock chemistry

The whole rock chemistry of samples used in the microstructural study was also analysed by the X-ray fluorescence method. These data and published analyses of Ploegsma (1989) (Table 1) from samples directly adjacent to the profile studied by the authors were used to construct a continuous geochemical profile from undeformed tonalite to ultramylonite. The chemical analysis of the sample showing the weakest degree of deformation was compared with tonalite

Table 1. Chemical composition of analysed samples

Sample	A	B	C	D	E	M	h27.1	h27.3	h1	h2	h4	h5	h6	h8
SiO_2	67.58	64.43	65.94	64.26	66.08	65.90	67.20	65.17	67.19	67.29	68.63	62.87	61.58	65.78
TiO_2	0.66	0.80	0.71	0.88	0.71	0.71	0.56	0.67	0.65	0.65	0.66	0.72	0.76	0.68
Al_2O_3	15.02	16.72	15.73	16.45	16.06	16.34	15.57	16.15	14.57	14.00	13.66	16.15	16.51	14.60
Fe_2O_3	0.38	0.24	0.15	0.18	0.19	0.18								
FeO	3.86	3.92	4.04	3.68	3.63	3.45	4.15*	4.57*	5.88*	5.63*	5.20*	6.56*	6.81*	5.90*
MnO	0.07	0.09	0.07	0.08	0.07	0.08	0.06	0.06	0.06	0.05	0.06	0.07	0.07	0.06
MgO	2.04	2.60	2.24	2.41	2.23	2.25	1.98	2.26	2.20	2.09	1.90	2.45	2.55	2.18
CaO	1.72	3.31	2.77	3.33	2.96	2.90	3.08	3.64	1.73	1.74	1.79	1.47	1.50	1.61
Na_2O	3.26	3.79	3.61	4.02	3.48	3.73	4.15	4.37	2.88	2.74	2.89	2.64	2.68	2.74
K_2O	3.79	2.25	2.07	2.26	2.16	2.12	2.68	2.65	4.72	4.72	3.99	6.66	6.83	5.10
P_2O_5	0.1	0.02	0.02	0.02	0.02	0.02	0.15	0.14	0.14	0.31	0.17	0.13	0.15	0.16
Total	99.90	99.79	99.82	99.74	99.83	99.76	99.56	100.21	100.21	99.69	99.44	100.38	100.02	99.25

Samples h27.1–h8 analysed by Ploegsma (1989), *FeO and Fe_2O_3 were not distinguished, all Fe is expressed as FeO tot. Correspondence of chemical analyses to samples from the figures: M ~ 5, E + D ~ 6, C ~ 7, B ~ 8, A ~ 9 + 10 + 11.

analyses of Ploegsma (1989) in order to establish the chemical homogeneity of the protolith.

The data are presented in weight-normalised form and plotted on the modified Gresens (1967) diagram (Potdevin and Marquer, 1987) which visually emphasises element gains and losses (Fig. 6). The lines in Fig. 6(b) show that the abundances of the mobile elements Ca, Na, K, Mg and Fe vary continuously with increasing degree of mylonitisation. These variations in element content are virtually negligible in the protomylonite and mylonite stage but they increase considerably in the ultramylonite, where the matrix volume is 70%.

The importance of migration of mobile elements with increasing deformation has been calculated by assuming Al_2O_3 was immobile (Grant, 1986; Kerrich *et al*., 1980; Marquer *et al*., 1985). The immobility of Al_2O_3 in deformed tonalites of Suomusjärvi shear zone was tested using Grant's (1986) isocon diagram. In the geochemical profiles three types of behaviour of the mobile elements can be defined: (1) CaO and Na_2O continuously decrease with increasing degree of mylonitisation, with a sharp gradient along the mylonite and ultramylonite boundary; (2) K_2O and Fe_2O_3 remain stable, or decrease slightly in the protomylonite- and mylonite stages, and abruptly increase at the transition from mylonite to ultramylonite; (3) MgO is fairly stable, increasing slightly in the mylonitic and ultramylonitic rocks.

Principal chemical changes in the mylonitised rocks are not associated with the increasing numbers of shear discontinuities but occur when the number of shear bands decreases during the ultramylonitic stage. This suggests that the fluids acted relatively late during shear zone evolution when more than 80% of ductile matrix was produced. The shear bands acted only as mechanical instabilities at intermediate strains and are not associated with chemical changes. Studies of permeability in ductile shear zones show that in weakly deformed *C–S* granites the porosity network is formed mainly by cracks, while in the ultramylonitic cores of shear zones the fluid transport is provided by a network of tubes along and across the foliation (Geraud *et al*., 1995). The relationships between strain softening during simple shear and fluid infiltration was numerically modelled by O'Hara (1994) assuming development of directed percolation clusters with high length/width ratios and anisotropic permeability. It follows that the increased permeability allows higher mobility of fluids within the ultramylonites, resulting in more efficient chemical mass transfer.

Mineral chemistry

Chemical changes in mylonitised rock should be attributed to the behaviour of all minerals involved in syntectonic mineral reactions taking place during mylonitisation (Kerrich *et al*., 1980; O'Hara, 1988). Chemical analyses of plagioclase porphyroclasts are shown in Fig. 7(a). The plagioclase crystals exhibit a composition of An_{30} and weak non-systematic zoning patterns. Microprobe analyses of ultrafine-grained light layers show enrichment in Ca and/or Na relative to the whole rock chemical analyses, indicating the persistent stability of ultrafine-grained plagioclase in the fine-grained matrix. Undistorted igneous biotite shows variations from 0.3 to 0.4 per formula unit (p.f.u.) of Ti and 3–4 p.f.u. of Fe (Fig. 7b). With increasing deformation, the Fe content decreases slightly up to 2.5–3 p.f.u. whereas Ti contents remain almost constant. Microprobe analyses of extremely dark areas in the ultrafine-grained matrix show enrichment in Fe, Mg and Ti contents indicating the local persistence of recrystallised biotite in the matrix.

Interpretation of the whole rock and mineral chemical compositions

The bulk rock chemistry changes are not accompanied by significant modifications in the mineral chemistry of relict clasts. The microprobe analyses of biotite and plagioclase clasts demonstrate the stability of these mineral phases throughout the course of de-

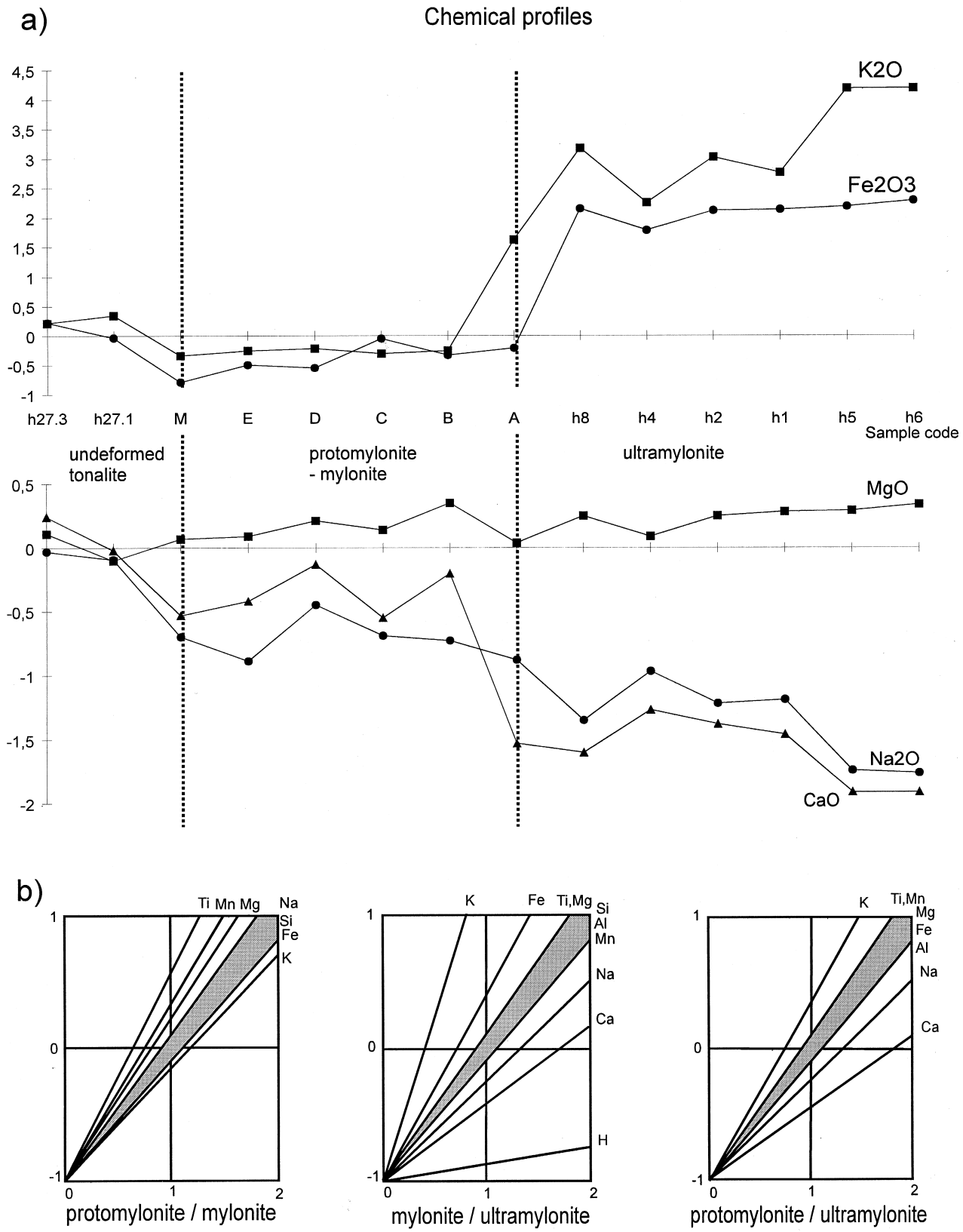

Fig. 6. (a) Geochemical profile through the Suomusjärvi shear zone and sequence of composition–volume diagrams (Potdevin and Marquer, 1987) based on weight-normalised element contents showing evolution of gains and losses with increasing deformation. Chemical analyses complemented by data of Ploegsma (1989) from the same locality (analyses h1–h27.3). (b) Gresens diagrams showing respective gains and losses of elements. Correspondence of chemical analyses to samples from the previous figures: M ~ 5, E + D ~ 6, C ~ 7, B ~ 8, A ~ 9 + 10 + 11.

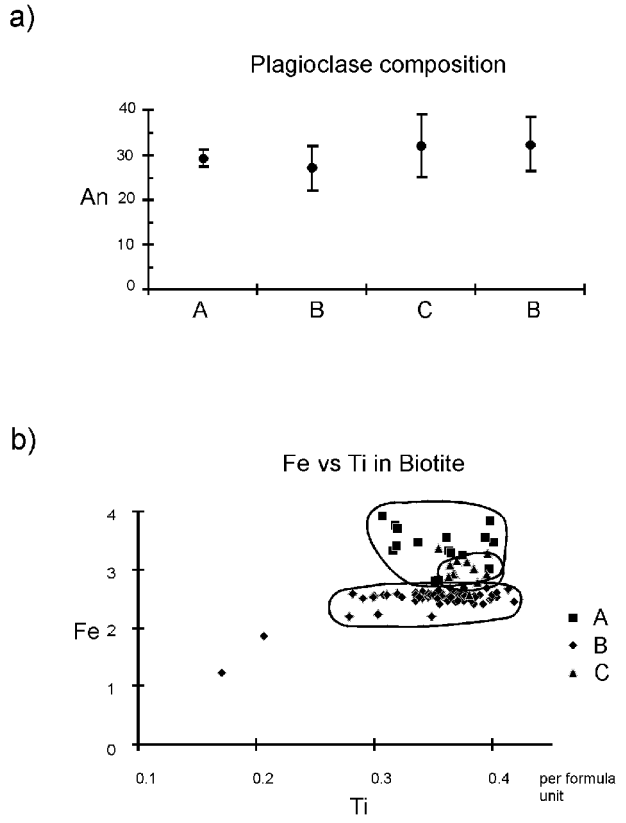

Fig. 7. Results of microprobe analyses of plagioclase and biotite. (a) Average and standard deviations of anorthite content in plagioclase, A—protomylonite, B—mylonite, C—ultramylonite. (b) Fe and Ti content in biotite clasts, A—protomylonite, B—mylonite, C—ultramylonite.

formation, with only minor and non-systematic changes in chemistry. Clasts along microshears did probably undergo chemical changes due to incipient recrystallisation and possible pressure solution but this cannot be tested in the present samples. This indicates that most of chemical changes within the mylonite occur in the ultrafine-grained matrix and are not associated with the origin of discontinuous shear instabilities. A slight decrease in CaO and Na_2O contents in both the protomylonite and mylonite indicates the beginning of destabilisation of plagioclase in the fine-grained matrix. A strong decrease in CaO and Na_2O and increase in Fe_2O_3 and K_2O in the ultramylonitic stage, assuming immobility of Al_2O_3, could be interpreted as an intense destabilisation of fine-grained plagioclase and relative increase in biotite volume in the matrix. Such chemical profiles are compatible with the infiltration of fluids channelised by the ultramylonitic shear zone during the later stages of shear zone evolution (Marquer, 1989).

GRAIN SIZE AND GRAIN ASPECT ANALYSIS

The results of feldspar clast grain size analysis is given in Fig. 8. Graph showing the values of arithmetic mean and standard deviation in an orthogonal system is presented in Fig. 9.

For protomylonites (Fig. 8a), the cumulative curve shows the relatively constant occurrence of size classes for small, medium and large grains up to a grain size equivalent of 100 mm^2. The average grain size is moderately high (21 mm^2), as is the standard deviation (Fig. 9). Relatively high aspect ratios for larger grains are characteristic of this protomylonitic stage. The smaller grains may have formed subsequently, but elongate grains with aspect ratios up to 5 do occur.

Mylonite (Fig. 8b) exhibits a marked decrease in the total number of clasts associated with a decrease in overall plagioclase volume (Fig. 4). The distribution of clast size up to 20 mm^2 is regular whereas the larger clasts rapidly decrease in number. The grain size statistics show a continuous decrease in average grain size and an associated decrease in standard deviation. The aspect ratio of the clasts also decreases, so that slightly elongate grains with average aspect ratios reaching 2 prevail.

At the ultramylonite stage (Fig. 8c) the total number and volume of clasts decrease to 12–15%. Small plagioclase clasts are most abundant, ranging from 0.5 to 4 mm^2 in size. A characteristic feature is the increase in average grain size associated with a decrease in standard deviation, indicating the disappearance of both the large clasts and small comminuted grains. An additional characteristic is a stabilisation of the aspect ratio of ovoid clasts of all sizes reaching an average value of 1.5.

GRAIN SHAPE ORIENTATION

Two methods were used to determine grain shape-preferred orientation: (1) orientation of long axes of feldspar clasts displayed in rose diagrams and (2) Panozzo's (1983, 1984) two-dimensional strain method (Fig. 10).

The tonalitic protomylonite exhibits a relatively strong preferred orientation of the whole set of feldspar grains, expressed as a typical bell-shaped form on Panozzo's diagram and a sharp maximum in the rose diagram (Fig. 10). The mylonitic stage is characterised by a flatter shape for the Panozzo graph and a weaker maximum on the rose diagram. The ultramylonite is characterised by a complete loss of preferred orientation of feldspar grain shape, marked by an almost flat shape to the Panozzo plot and an indistinct maximum in the rose diagram. These data show that the intensity of grain shape-preferred orientation progressively diminishes towards the core of the shear zone.

DISCUSSION

The Suomusjärvi shear zone provides the opportunity for studying successive stages of tonalite defor-

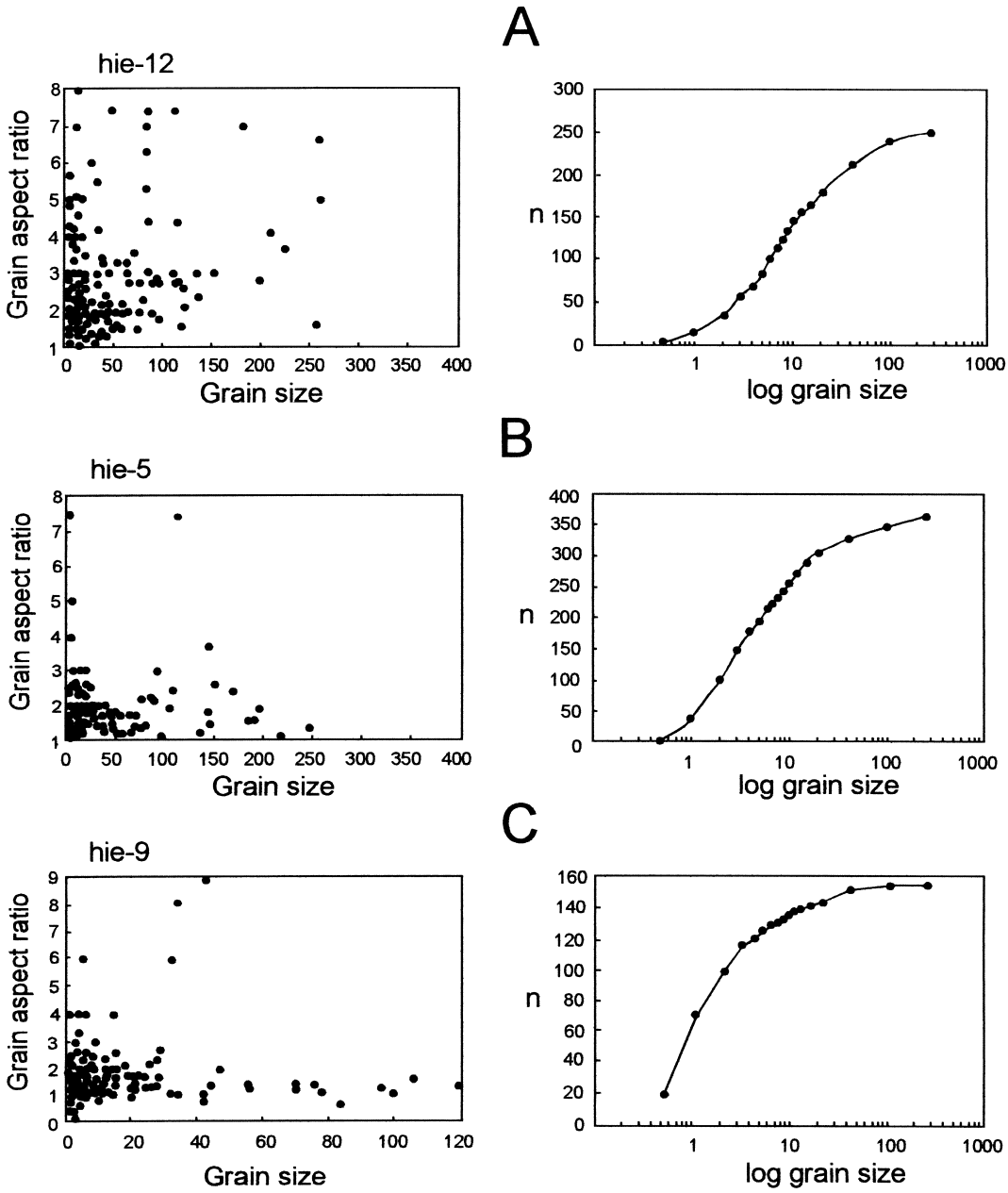

Fig. 8. Diagrams showing representative results of grain size and aspect ratio analysis. Left column shows orthogonal diagrams of grain aspect ratio vs grain size. Right column shows logarithmic cumulative grain size curves. A—protomylonite, B—mylonite, C—ultramylonite. The measurements were made in this section.

mation from undeformed tonalite to ultramylonite via protomylonite with 20% ductile matrix and mylonite with 80% matrix.

The tonalite, unaffected by late shear deformation, exhibits sub-solidus microstructures and an intense magmatic preferred orientation of feldspars and micas. Feldspar contiguity is very weak and the majority of plagioclase phenocrysts are surrounded by biotite and quartz grains, which represent about 45% of the whole rock composition. Since the rigid minerals were not interconnected prior to deformation, the stability field of the load-bearing structure (LBF) was restricted from the very beginning (Handy, 1990, 1994).

The protomylonite is characterised by the presence of 55% feldspar clasts surrounded by an anastomosing network of conjugate shear bands affecting quartz and biotite. The deformation of plagioclase is characterised by fracturing or by the development of zones of dynamically recrystallised small grains. Plagioclase clasts show strong grain size variation, large aspect ratios and intense grain-shape preferred orientation.

At this stage, quartz deforms plastically; it is recrystallised and exhibits characteristic grain size variations around rigid plagioclase clasts. Intense grain size reduction of quartz in neck zones between rigid plagioclase clasts indicates high stress and strain partitioning

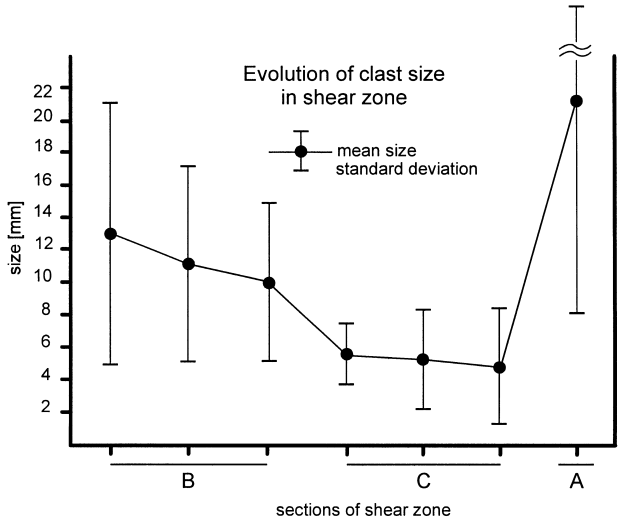

Fig. 9. Diagram showing relationship between average grain size of clasts and standard deviation for different stages of mylonitisation through the Suomusjärvi shear zone.

(Handy, 1990, 1994) controlled by plagioclase clast spacing. Biotite shows signs of kinking, intense dynamic recrystallisation and grain size reduction down to several microns. These microstructures could be interpreted as an interconnected weak layer structure (IWL) in which plagioclase represents the strong phase, with quartz and biotite as weak phases. Strain concentration in weak phases is typical of an IWL structure with a relatively low proportion of weak phases and a strong viscosity contrast between the strong and the weak phases (Fig. 11). The bulk rock chemistry does not change much relative to the original tonalite during this stage, with the exception of minor decreases in CaO and Na_2O. This is probably due to the low porosity of weakly deformed *C–S* granitoids (Geraud *et al.*, 1995). The chemical composition of relic plagioclase and biotite clasts remains constant. This indicates that deformation was isochemical and governed by the development of mechanical instabilities in weak phases.

The mylonitic stage is characterised by a decrease in plagioclase clast volume down to 35–40%, an almost doubling of the number of clasts, a decrease in the density of shear bands and an increase in volume of fine-grained matrix. Plagioclase is strongly fractured but also shows signs of plastic deformation marked by strain-induced twinning and dynamic recrystallisation at relict clast margins. Early fracturing and later dynamic recrystallisation lead to progressive grain size reduction and increase in the number of clasts. The fractured feldspar clasts are mostly smaller than 20 mm^2 and have aspect ratios less than 2. Such fracturing of feldspars enhances later dislocation creep deformation at constant temperature (Tullis and Yund, 1987). Both processes contribute to the formation of a fine-grained matrix and to strain weakening in the mylonite. The volume of finely recrystallised grains becomes large enough in conjunction with other minerals to constitute an interconnected network. Quartz, present as elongated folded ribbons composed of subequent small grains, shows a strong decrease in volume to 2–5%, and relict biotite almost disappears. Dark ultra-fine-grained matrix, affected by a small number of shear instabilities, reaches 50–60%. A major change in deformation mechanism to grain boundary sliding starts to occur in the weak matrix when the fracturing of rigid feldspar clasts reaches its maximum. The rheological evolution of the rock is characterised by a transition from the IWL structure, with a low proportion of the weak phases and a strong viscosity contrast, to an IWL structure with high amounts of weak phase (Fig. 11). Chemical changes are not important and are marked only by decreasing whole rock CaO and Na_2O contents, whereas biotite and plagioclase compositions remain stable. This may indicate the continuous dissolution of small plagioclase grains within a weak matrix.

Ultramylonite shows a decrease in plagioclase clast volume down to 12%, the disappearance of quartz and biotite, the absence of heterogeneous shear bands and an increase in matrix volume. Clast size decreases to 10 mm and shows a homogeneous size distribution. All recrystallised plagioclase grains disappear through continuous recrystallisation and large clasts fracture and approach a uniform equilibrium size. The clast aspect ratio becomes uniform, so that all grains have an almost constant aspect ratio of 1.5, regardless of size. Feldspar clasts no longer show any grain shape-preferred orientation. Chemical analyses of ultramylonite show a strong decrease in CaO and Na_2O contents and an increase in Fe_2O_3 and K_2O concentrations due to breakdown of feldspars. Microprobe analyses of relic plagioclase clasts exhibit no changes in their chemistry, probably reflecting the importance of fine-grained recrystallised plagioclase dissolution in the matrix associated with relative biotite enrichment. Such reaction softening may enhance the ductility of fine-grained micaceous matrix (Mitra, 1978; White *et al.*, 1980). The geochemical data suggest that the fluids infiltrated the shear zone at a relatively late stage of shear zone evolution when well localised ultramylonitic zones already existed. It is suggested that if volume loss occurred during deformation then the permeability can substantially increase during deformation (O'Hara, 1990, 1994).

There are several lines of evidence indicating that the ultramylonitic microstructure is a steady-state structure. Means (1981) cited several criteria as diagnostic of steady-state foliation: (1) cyclicity of structural changes in a given sub-region, (2) reduction in aspect ratio of grains and (3) destruction of mineralogical layering. We propose that in the Suomusjärvi shear zone all these requirements are fulfilled.

The ultrafine-grained matrix grains are only several microns in size allowing effective grain boundary sliding (Boullier and Gueguen, 1978; Kerrich *et al.*, 1980)

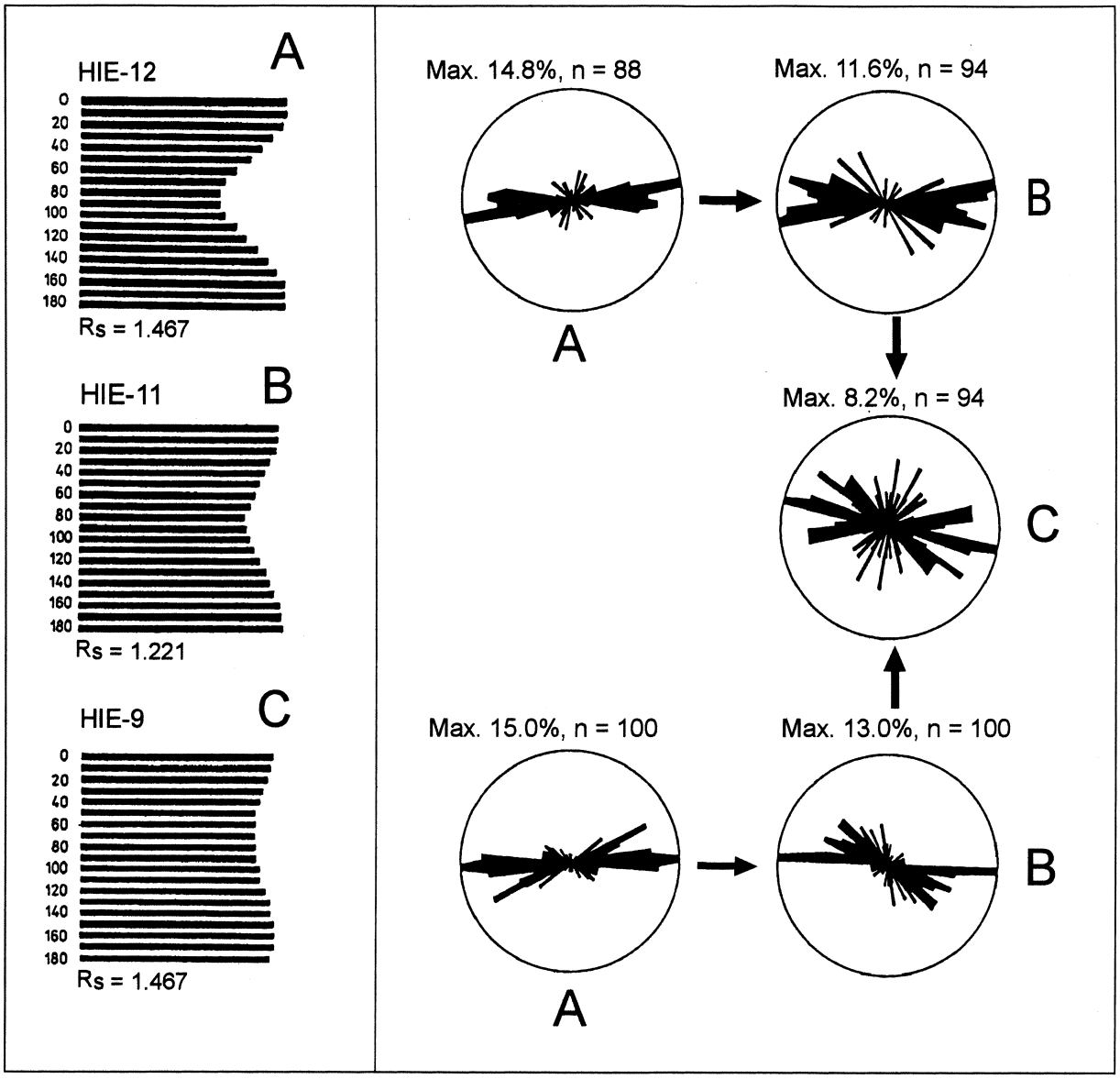

Fig. 10. Results of representative grain-shape orientation analyses. Left column show Panozzo's diagrams based on projections of grain contours on a horizontal axis. Right column show rose diagrams of clast long axes. (A)—protomylonite, (B)—mylonite, (C)—ultramylonite.

of the ductile matrix. Plagioclase clasts also exhibit significant grain size and grain aspect reduction. The lack of preferred orientation of plagioclase clasts is interpreted to result from rigid body rotation of feldspar clasts in a very ductile matrix similar to the movement of rigid inclusions in a slowly moving Newtonian fluid. The low volume of clasts (10–12%) will permit their unimpeded movement. Such a preferred orientation of rigid ellipsoidal inclusions is virtually cyclical and a typical feature of multiparticle systems within a simple shear flow regime (Fernandez and Laporte, 1991; Ježek *et al.*, 1994). According to numerical modelling of Ježek *et al.* (1994), using Jeffery's (1922) equation, the particles with an axial ratio of 2 moving within a slowly moving viscous medium, will lose any preferred orientation after a period corresponding to $\gamma = 8.2$. Consequently, a minimum shear strain greater than $\gamma = 8$, but probably much higher, is necessary to produce such a weak shape-preferred orientation, provided that the original orientation of the particles was random. A larger γ (about 15–20) is required for multiparticle systems starting with an original preferred orientation in order to destroy this preferential alignment. The loss of grain shape-preferred orientation, loss of aspect ratio and cyclicity of particle movements based on Jeffery's model are therefore typical features of steady-state flow conditions in Suomusjärvi ultramylonites.

Stress considerations

Variations in quartz grain size at the protomylonite stage indicate strong stress concentrations in weak minerals, depending on the spacing and size of large

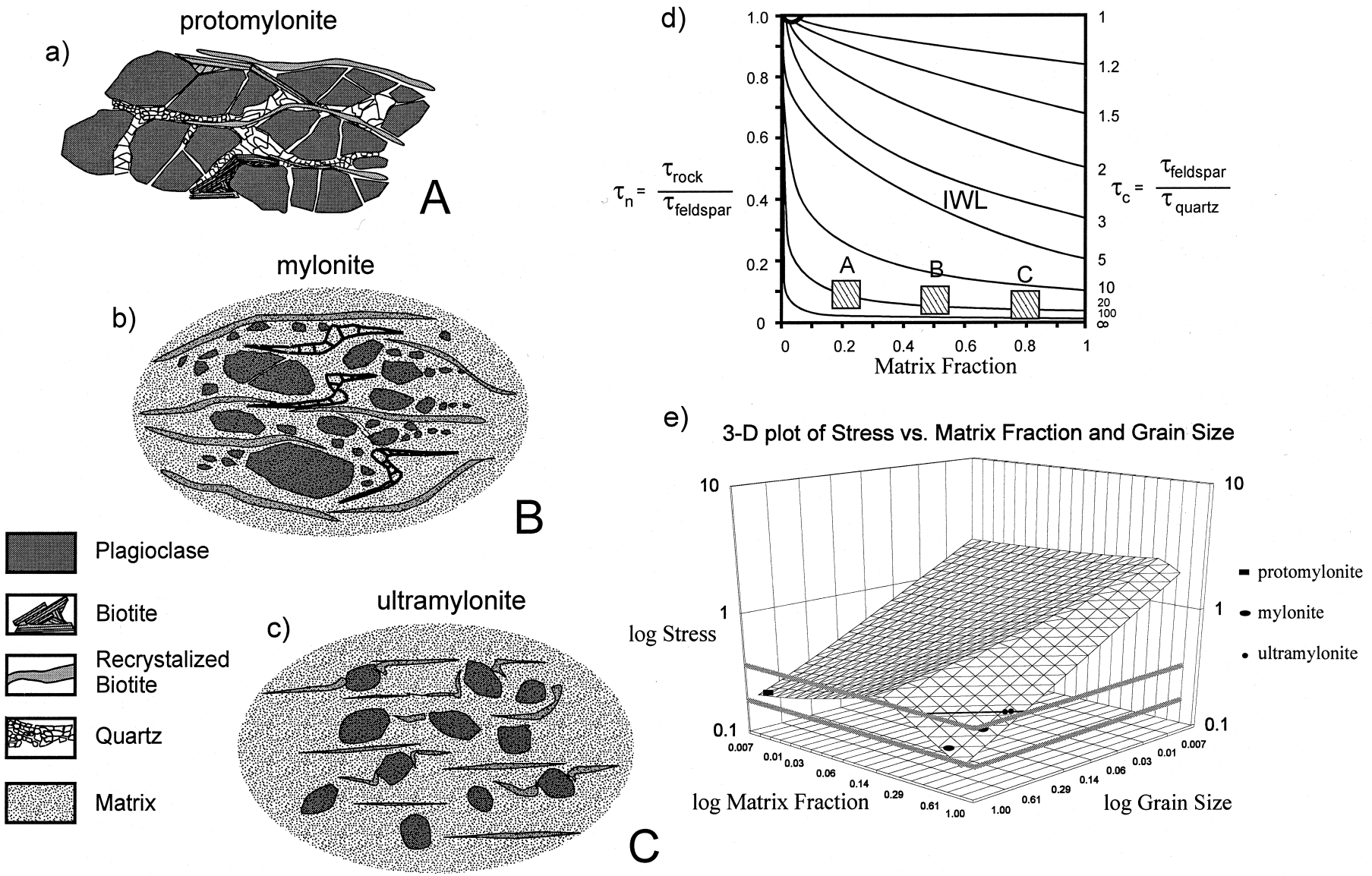

Fig. 11. Left column of drawings (a–c) shows main microstructural features of deformed tonalite from protomylonite A, to mylonite B and ultramylonite C. (d) Matrix–clast relationships expressed on structural diagram of Handy (1994) showing relationship between amount of weak matrix and viscosity ratio between plagioclase and weak matrix. (e) 3D logarithmic diagram of stress necessary for grain fracturing vs normalised clast size and normalised proportion of matrix fraction. Modified after Mitra (1978).

feldspar clasts. With increasing deformation, the shear heterogeneities disappear and stress and deformation are distributed homogeneously throughout the matrix. The increase of matrix proportion is related to a decrease in stress and strain rate concentration (Handy, 1990, 1994). The grain-size reduction of all mineral phases enhances the ductility of the weak matrix which accordingly accommodates a greater proportion of the strain and exerts a large weakening effect on the bulk strength of the whole rock (Handy, 1990).

Mitra (1978) summarised fracture mechanisms at low and high matrix percentages, showing that the stress necessary to initiate a crack in a brittle grain above a certain size depends on grain size (d), characteristic depth in the grain at which the concentrated stress is achieved (l), and on the amount of weak matrix (fm). Using equations (10) and (15) of Mitra (1978) an estimation of non-dimensional critical stress (snd) necessary for grain cracking at low and high matrix percentages can be made. This stress necessary for grain cracking decreases with an increasing matrix volume at constant grain size at high matrix fractions and increases with decreasing grain size (Fig. 11e). In the Suomusjärvi shear zone, the amount of weak matrix continuously decreases in conjunction with the mean clast size.

Figure 11(e) shows that the stress level necessary for crack initiation continuously increases up to very high percentages of weak matrix. At the final stage, when the size of small clasts and the amount of weak matrix reaches a critical value, a significant increase in stress is necessary for further cracking to occur. The size of relict clasts in the shear zone core is thus in equilibrium with the stabilised stress level reached under steady-state conditions.

CONCLUDING REMARKS

Major differences in deformation mechanisms occurred across the transition from mylonite to ultramylonite strain states in the Suomusjärvi shear zone:

(1) The deformation was first governed by crystal plasticity in quartz and biotite and by fracturing accompanied by minor recrystallisation of plagioclase. Strain was concentrated along a network of anastomosing shear bands with high stress and strain rate concentration responsible for continuous fracturing of feldspars. Deformation was not accompanied by significant chemical mass transfer during this stage and it is probable that the sheared region progressively widened during this stage, behaving as a type I shear zone of Means (1995).

(2) An increase in the amount of weak matrix lead to isolation of small feldspars, disappearance of quartz and to the progressive disappearance of shear bands. At this stage the matrix behaved superplastically and relict feldspars clasts were free to rotate in a viscous matrix medium. The feldspar clast size decreased by dynamic recrystallisation and probably also by dissolution at highly stressed margins. Major changes in chemistry occurred corresponding to dissolution of plagioclase in the matrix. Steady state flow conditions were attained in the core of the Suomusjärvi shear zone and were associated with decrease in stress and strain rate concentration. Dynamic equilibrium between clast number, size and proportion with respect to ductile matrix is characteristic for this strain state. Deformation became progressively localised in a zone channel with a high viscosity contrast with respect to the weakly deformed margins which became inactive with time.

Acknowledgements—Financial support of the Czech National Foundation grant No. 30 709 is acknowledged. We are grateful to Professor Ilmari Haapala and Dr Mikko Nironen for their support and help. The reviews of Didier Marquer, Kieran O'Hara and Peter Sorjonen Ward are highly appreciated.

REFERENCES

Blumenfeld, P., Mainprice, D. and Bouchez, J. L. (1986) C-slip in quartz from subsolidus deformed granite. *Tectonophysics* **127,** 97–115.

Boullier, A. M. and Gueguen, Y. (1978) SP-mylonites: origin of some mylonites by superplastic flow. *Contributions to Mineralogy and Petrology* **50,** 93–104.

Burg, J. P. and Laurent, P. (1978) Strain analysis of a shear zone in granodiorite. *Tectonophysics* **47,** 15–42.

Etheridge, M. A., Wall, V. J. and Cox, S. F. (1984) High fluid pressures during regional metamorphism and deformation: implication for mass transport and deformation mechanisms. *Journal of Geophysical Research* **89,** 4344–4358.

Fernandez, A. and Laporte, D. (1991) Significance of low symmetry fabrics in magmatic flows. *Journal of Structural Geology* **13,** 337–347.

Gaál, G. and Gorbatschev, R. (1987) An outline of the Precambrian evolution of the Baltic shield. *Precambrian Research* **35,** 15–52.

Gapais, D. (1989a) Les orthogneiss; Structures, mécanismes de déformation et analyse cinématique. (Exemple du granite de Flamanville.). *Mémoires et Documents du Centre Armoricain d'Etude Structurale des Socles*.

Gapais, D. (1989b) Shear structures within deformed granites: mechanical and thermal indicators. *Geology* **17,** 1144–1147.

Geraud, Y., Caron, J. and Faure, P. (1995) Porosity network of a ductile shear zone. *Journal of Structural Geology* **17,** 1757–1769.

Grant, J. A. (1986) The isocon diagram—a simple solution to Gresen's equation for metasomatic alteration. *Economic Geology* **81,** 1976–1982.

Gresens, R. L. (1967) Composition volume relations of metasomatism. *Chemical Geology* **2,** 47–65.

Handy, M. R. (1990) The solid state flow of polymineralic rocks. *Journal of Geophysical Research* **95,** 8647–8661.

Handy, M. R. (1994) Flow laws for rocks containing two non-linear viscous phases: a phenomenological approach. *Journal of Structural Geology* **3,** 287–301.

Hirth, G. and Tullis, J. (1992) Dislocation creep regimes in quartz aggregates. *Journal of Structural Geology* **14,** 145–160.

Huhma, H. (1986) Sm–Nd, U–Pb and Pb–Pb isotopic evidence for the origin of the Early Proterozoic Svecokarelian crust in Finland. *Bulletin of the Geological Survey of Finland* **337,** 48 p.

Hull, J. (1988) Thickness–displacement relationships for deformation zones. *Journal of Structural Geology* **10,** 431–435.

Jeffery, G. B. (1922) The motion of ellipsoidal particles immersed in a viscous fluid. *Proceedings of the Royal Society of London, Series A* **102,** 161–179.

Ježek, J., Melka, R., Schulmann, K. and Venera, Z. (1994) The behaviour of rigid triaxial ellipsoidal particles in viscous flows—modelling of fabric evolution in a multiparticle system. *Tectonophysics* **229,** 165–180.

Jordan, P. G. (1987) The deformational behaviour of bimineralic limestone-halite aggregates. *Tectonophysics* **135,** 185–197.

Jordan, P. G. (1988) The rheology of polymineralic rocks—an approach. *Geologische Rundschau* **77,** 285–294.

Kerrich, R., Allison, I., Barnett, R., Moss, S. and Starkey, J. (1980) Microstructural and chemical transformations accompanying deformation of granite in a shear zone at Milléville, Switzerland; With implications for stress corrosion cracking and superplastic flow. *Contributions to Mineralogy and Petrology* **73,** 221–242.

Marquer, D., Gapais, D. and Capdevila, R. (1985) Comportement chimique et orthogneissification d'une granodiorite en faciés verts (Massif de l'Aar, Alpes centrales). *Bulletin de Minéralogie* **108,** 209–221.

Marquer, D. (1987) Transfert de matière et déformation progressive des granitoides. Exemple des massifs de l'Aar et du Gothard (Alpes centrales suisses). *Mémoires et Documents du Centre Armoricain d'Etude Structurale des Socles, Rennes* **10**.

Marquer, D. (1989) Transfert de matiere et deformation des granitoides, aspect methodologiques. *Schweizerische Mineralogie Petrographische Mitteilungen* **69,** 15–35.

Marquer, D. and Burkhard, M. (1992) Fluid circulation, progressive deformation and mass-transfer processes in the upper crust: the example of basement-cover relationships in the External Crystalline Massifs, Switzerland. *Journal of Structural Geology* **14,** 1047–1057.

Means, W. D. (1981) The concept of steady state foliation. *Tectonophysics* **78,** 179–199.

Means, W. D. (1995) Shear zones and rock history. *Tectonophysics* **247,** 157–160.

Melka, R., Schulmann, K., Schulmannová, B., Hrouda, F. and Lobkowicz, M. (1992) The evolution of perpendicular linear fabrics in a synkinematically emplaced tourmaline granite (central Moravia—Bohemian Massif). *Journal of Structural Geology* **14,** 605–620.

Mitra, G. (1978) Ductile deformation zones and mylonites: the mechanical processes involved in the deformation of crystalline basement rocks. *American Journal of Science* **278,** 1057–1084.

Mitra, G. (1992) Deformation of granitic basement rocks along fault zones at shallow to intermediate crustal levels. In *Structural Geology of Fold and Thrust Belts*, ed. S. Mitra and G. W. Fisher, pp. 123–144. John Hopkins University Press, Baltimore, MD.

O'Hara, K. D. (1988) Fluid flow and volume loss during mylonitisation: A origin of phyllonite in an overthrust setting, North Carolina, U.S.A. *Tectonophysics* **156,** 21–36.

O'Hara, K. D. (1990) State of strain in mylonites from the western Blue Ridge province, southern Appalachians: The role of volume loss. *Journal of Structural Geology* **12,** 419–430.

O'Hara, K. D. (1994) Fluid–rock interaction in crustal shear zones: A directed percolation approach. *Geology* **22,** 843–846.

Panozzo, R. (1983) Two-dimensional analysis of shape fabric using projections of digitised lines in a plane. *Tectonophysics* **212,** 279–294.

Panozzo, R. (1984) Two-dimensional strain from the orientation of lines in a plane. *Journal of Structural Geology* **6,** 215–221.

Potdevin, J-L. and Marquer, D. (1987) Metode de quantification de transferes de matiere par les fluides dans les roches métamorphiques deformées. *Geodinamica Acta* **1,** 193–206.

Ploegsma, M. (1989) Shear zones in the West Uusimaa area, SW Finland. Ph.D. thesis, Vrije Universiteit Amsterdam.

Schmid, S. M. (1982) Microfabric studies as indicators of deformation mechanisms and flow laws operative in mountain building. In *Mountain Building Processes*, ed. K. Hsu.

Schmid, S. M. and Handy, M. R. (1991) Towards a genetic classification of fault rocks: geological usage and tectonophysical implications. In *Controversies in Modern Geology*. Academic Press.

Schreurs, J. and Westra, L. (1986) The thermometric evolution of a Proterozoic, low pressure, granulite dome, West Uusimaa, SW Finland. *Contributons to Mineralogy and Petrology* **93,** 236–250.

Schulmann, K., Mlčoch, B. and Melka, R. (1996) High-temperature microstructures and rheology of deformed granite, Erzgebirge, Bohemian Massif. *Journal of Structural Geology* **18,** 719–733.

Tullis, J. and Yund, R. A. (1987) Transition from cataclastic flow to dislocation creep of feldspar: Mechanisms and microstructures. *Geology* **15,** 606–609.

Urai, J. L., Means, W. D. and Lister, G. S. (1986) Dynamic recrystallisation of minerals. In *Mineral and rock deformation: Laboratory studies (The Paterson Volume)*, eds B. E. Hobbs and H. C. Heard. American Geophysical Union Geophysical Monograph **36,** pp. 161–200.

White, S. H. (1976) The effects of strain on the microstructures, fabrics and deformation mechanism in quartzites. *Philosophical Transactions of the Royal Society of London* **A. 283,** 69–86.

White, S. H. and Knipe, R. J. (1978) Transformation and reaction enhanced ductility in rocks. *Journal of the Geological Society of London* **135,** 513–516.

White, S. H., Burrows, S. E., Carreras, J., Shaw, N. D. and Humpreys, F. J. (1980) On mylonites in ductile shear zones. *Journal of Structural Geology* **2,** 175–187.